Theor Chem Acc (2003) 110:49–58
DOI 10.1007/s00214-003-0456-0

Theoretical
Chemistry Accounts

Feature article

Simulating quantum dynamics in classical environments

Alessandro Sergi[1], **Donal Mac Kernan**[2], **Giovanni Ciccotti**[3], **Raymond Kapral**[1]

[1] Chemical Physics Theory Group, Department of Chemistry, University of Toronto, Toronto, ON M5S 3H6, Canada
[2] Department of Physics and Centre for Scientific Computation, Trinity College, Dublin 2, Ireland
[3] INFM and Dipartimento di Fisica, Università "La Sapienza", Piazzale Aldo Moro, 2, 00185 Rome, Italy

Received: 6 March 2003 / Accepted: 6 May 2003 / Published online: 11 August 2003

Abstract. Methods for simulating the dynamics of composite systems, where part of the system is treated quantum mechanically and its environment is treated classically, are discussed. Such quantum–classical systems arise in many physical contexts where certain degrees of freedom have an essential quantum character while the other degrees of freedom to which they are coupled may be treated classically to a good approximation. The dynamics of these composite systems are governed by a quantum–classical Liouville equation for either the density matrix or the dynamical variables which are operators in the Hilbert space of the quantum subsystem and functions of the classical phase space variables of the classical environment. Solutions of the evolution equations may be formulated in terms of surface-hopping dynamics involving ensembles of trajectory segments interspersed with quantum transitions. The surface-hopping schemes incorporate quantum coherence and account for energy exchanges between the quantum and classical degrees of freedom. Various simulation algorithms are discussed and illustrated with calculations on simple spin-boson models but the methods described here are applicable to realistic many-body environments.

Keywords: Nonadiabatic dynamics – Quantum–classical dynamics – Surface hopping – Open quantum systems

1 Introduction

It is difficult to simulate the dynamics of quantum many-body systems. Although it is possible to perform classical molecular dynamics simulations of condensed phase and complex systems, many problems cannot be treated accurately using classical mechanics. One way to treat problems of this type is to adopt an approach based on mixed quantum–classical dynamics where part of the system is treated classically and the remainder of the system is treated quantum mechanically. Proton and electron transfer processes, ubiquitous in chemical and biochemical systems, are two examples of systems where such a quantum–classical approach may be useful.

Approximations based on mixed quantum–classical dynamics are well known [1, 2, 3] and many different approaches using this idea have been constructed. These include methods employing path integral formulations of quantum mechanics [4], mean-field approximations to the quantum dynamics [5, 6], various semiclassical approximations [7] as well as methods based on surface-hopping schemes [8, 9, 10]. Quantum–classical methods involve classical phase space degrees of freedom of the environment or bath (R, P) and represent the quantum degrees of freedom in a suitable set of basis states. Often adiabatic or Born–Oppenheimer states that depend parametrically on the bath coordinates, R, are used to represent the quantum subsystem in mean-field and surface-hopping methods. In mean-field approximations the evolution is determined by mean forces that are calculated from the expectation value of the potential using the instantaneous value of the system wave function. In most surface-hopping schemes the classical evolution takes place on single adiabatic potential-energy surfaces, interspersed by quantum transitions.

In this article we discuss an approach to nonadiabatic mixed quantum–classical dynamics based on a quantum–classical Liouville equation. In Sect. 2 we sketch how this evolution equation can be obtained from the quantum mechanical von Neumann equation for the density matrix by taking a partial Wigner transform and performing an expansion of the evolution operator in a small parameter determined by the ratios of the masses of the quantum and classical particles. The abstract evolution equations are written in terms of subsystem and adiabatic bases in Sect. 3. The formal solutions of the evolution equations are given in Sect. 4, while some details concerning the computation of the part of the evolution operator responsible for nonadiabatic

Correspondence to: R. Kapral
e-mail: rkapral@gatto.chem.utoronto.ca

dynamics are presented in Sect. 5. The results are illustrated by simulations on spin-boson systems in Sect. 6 and the conclusions of the paper are given in Sect. 7.

2 Quantum–classical equations of motion

Suppose that a system can be partitioned into a set of quantum mechanical degrees of freedom and a set of classical environmental degrees of freedom. In isolation from each other each of these two sets of degrees of freedom evolves according to the well-known equations of quantum and classical mechanics. In the approach discussed in this paper, the dynamics of the composite quantum–classical system are described by the Liouville equation,

$$\begin{aligned}\frac{\partial\hat{\rho}_{\rm W}(R,P,t)}{\partial t} &= -\frac{i}{\hbar}[\hat{H}_{\rm W},\hat{\rho}_{\rm W}(t)] \\ &\quad+\frac{1}{2}\Big(\{\hat{H}_{\rm W},\hat{\rho}_{\rm W}(t)\}-\{\hat{\rho}_{\rm W}(t),\hat{H}_{\rm W}\}\Big) \\ &= -[\hat{H}_{\rm W},\hat{\rho}_{\rm W}(t)] = -i\hat{\mathscr{L}}\hat{\rho}_{\rm W}(t)\ , \end{aligned} \tag{1}$$

that gives the time evolution of the density matrix $\hat{\rho}_{\rm W}(R,P,t)$ expressed in the partial Wigner representation introduced later [11, 12, 13, 14, 15, 16, 17, 18]. The subscript W denotes this partial Wigner transform. The corresponding equation of motion for an observable $\hat{A}_{\rm W}(R,P,t)$ is [17]

$$\frac{{\rm d}\hat{A}_{\rm W}(R,P,t)}{{\rm d}t} = [\hat{H}_{\rm W},\hat{A}_{\rm W}(t)] = i\hat{\mathscr{L}}\hat{A}_{\rm W}(t)\ . \tag{2}$$

The last lines in these equations define the quantum–classical bracket for any two operators $(\hat{A}_{\rm W},\hat{B}_{\rm W})$ and the Liouville operator $\hat{\mathscr{L}}$ [17, 19]. Both the density matrix and the observable are operators in the Hilbert space of the quantum degrees of freedom and functions of the phase space coordinates (R,P) of the classical environment. To simplify the notation we drop the dependence on the classical phase space variables when confusion is unlikely to arise. In these equations $[\cdot,\cdot]$ is the commutator and $\{\cdot,\cdot\}$ is the Poisson bracket. The Hamiltonian $\hat{H}_{\rm W}(R,P)$ of the system is

$$\hat{H}_{\rm W}(R,P) = \frac{P^2}{2M}+\frac{\hat{p}^2}{2m}+\hat{V}_{\rm W}(\hat{q},R)\ , \tag{3}$$

and consists of the sum of the kinetic energy of the classical particles, $P^2/2M$, the kinetic energy operator for the quantum degrees of freedom, $\hat{p}^2/2m$, and the total potential-energy operator, $\hat{V}_{\rm W}(\hat{q},R)=\hat{V}_{\rm s}(\hat{q})+V_{\rm b}(R)+\hat{V}_{\rm c}(\hat{q},R)$, which describes all interactions within the quantum (s) and classical bath (b) subsystems as well as the interactions (c) between the subsystems. Henceforth, the hats will be used to denote quantum operators.

An examination of Eqs. (1) and (2) shows that if the classical environment is not present, Eq. (1) reduces to the quantum Liouville equation for the quantum subsystem,

$$\frac{\partial\hat{\rho}_{\rm s}(t)}{\partial t} = -\frac{i}{\hbar}[\hat{H}_{\rm s},\hat{\rho}_{\rm s}(t)]\ , \tag{4}$$

where the quantum subsystem Hamiltonian is $\hat{H}_{\rm s}=\frac{\hat{p}^2}{2m}+\hat{V}_{\rm s}(\hat{q})$, while Eq. (2) becomes the Heisenberg equation of motion. Similarly, if the quantum subsystem is not present one obtains the classical Liouville equation,

$$\frac{\partial\rho_{\rm b}(R,P,t)}{\partial t} = \{H_{\rm b}(R,P),\rho_{\rm b}(R,P,t)\}\ , \tag{5}$$

where the classical bath Hamiltonian is$H_{\rm b}(R,P)=\frac{P^2}{2M}+V_{\rm b}(R)$, and Eq. (2) takes the form of the classical evolution equation for a bath dynamical variable.

In Eq. (1), the coupling between these two subsystems appears in both terms in the quantum–classical Liouville operator since $\hat{V}_{\rm W}(\hat{q},R)$ accounts for interactions between the two subsystems. The quantum character manifests itself in the Poisson bracket terms since the quantum operators do not commute and their order must be respected. This feature along with the properties of the commutator imply that the right-hand sides of Eqs. (1) and (2) are antisymmetric, an important property guaranteeing energy conservation, as can be seen by letting $\hat{A}_{\rm W}=\hat{H}_{\rm W}$ in Eq. (2). Some quantum–classical evolution equations with similar structure [20, 21] do not satisfy this antisymmetry property and difficulties with such approaches have been noted [22].

The derivation of Eq. (1) starts with the von Neumann equation,

$$\frac{\partial\hat{\rho}}{\partial t} = -\frac{i}{\hbar}[\hat{H},\hat{\rho}]\ , \tag{6}$$

for a quantum system comprising two quantum subsystems with light, m, and heavy, M, masses and coordinate and momentum operators $(\hat{q},\hat{p})$ and $(\hat{Q},\hat{P})$, respectively. The full quantum Hamiltonian operator then takes the form, $\hat{H}=\hat{P}^2/2M+\hat{p}^2/2m+\hat{V}(\hat{q},\hat{Q})$. The heavy-mass degrees of freedom will ultimately be treated classically and constitute the environment for the quantum subsystem.

To treat only the environmental degrees of freedom classically, it is convenient to take a partial Wigner transform of Eq. (6) over the $3N$ heavy-mass degrees of freedom,

$$\hat{\rho}_{\rm W}(R,P) = (2\pi\hbar)^{-3N}\int{\rm d}z\,{\rm e}^{iP\cdot z/\hbar}\Big\langle R-\frac{z}{2}|\hat{\rho}|R+\frac{z}{2}\Big\rangle\ . \tag{7}$$

The subscript W refers to this partial Wigner transform [23]. Similarly, the partial Wigner transform of an operator $\hat{A}$ is

$$\hat{A}_{\rm W}(R,P) = \int{\rm d}z\,{\rm e}^{iP\cdot z/\hbar}\Big\langle R-\frac{z}{2}|\hat{A}|R+\frac{z}{2}\Big\rangle\ . \tag{8}$$

To take the quantum–classical limit in Eq. (6) we scale the variables so that the momenta of the heavy particles have the same magnitude as those of the light particles, μP, where $\mu=(m/M)^{1/2}$, and measure all distances in length units appropriate for the quantum subsystem [17, 24].[1] Letting energy be measured in terms of the energy unit, ϵ_0, time in units of $t_0=\hbar/\epsilon_0$ and length in units of

[1] A quantum-classical description of a system can also be justified by arguments based on decoherence

$\lambda_m = (\hbar^2/m\epsilon_0)^{1/2}$, the momentum units are selected to be $p_m = (m\lambda_m/t_0) = (m\epsilon_0)^{1/2}$ and $P_M = (M\epsilon_0)^{1/2}$. To proceed we make use of the rule for the Wigner transform of a product of operators [23]

$$(\hat{A}\hat{B})_{\rm W} = \hat{A}_{\rm W} {\rm e}^{\hbar\Lambda/2i} \hat{B}_{\rm W} \ , \tag{9}$$

where the operator Λ is the negative of the Poisson bracket operator,

$$\Lambda = \overleftarrow{\nabla}_P \cdot \overrightarrow{\nabla}_R - \overleftarrow{\nabla}_R \cdot \overrightarrow{\nabla}_P \ , \tag{10}$$

and the direction of an arrow indicates the direction in which the operator acts. Using this result, the partial Wigner transform of Eq. (6), when expressed in the scaled units, $\hat{q}' = \hat{q}/\lambda_m$, $R' = R/\lambda_m$, $\hat{p}' = \hat{p}/p_m$, $P' = P/P_M$ and $t' = t/t_0$, takes the form

$$\frac{\partial \hat{\rho}'_{\rm W}(R',P',t)}{\partial t'} = -i\Big[\hat{H}'_{\rm W} {\rm e}^{\mu\Lambda'/2i} \hat{\rho}'_{\rm W}(t') - \hat{\rho}'_{\rm W}(t') {\rm e}^{\mu\Lambda'/2i} \hat{H}'_{\rm W}\Big] \ . \tag{11}$$

Expanding the right-hand side of Eq. (11) to first order in the small parameter $\mu = (m/M)^{1/2}$ one finds

$$\frac{\partial \hat{\rho}'_{\rm W}(R',P',t)}{\partial t'} = -i\left[\hat{H}'_{\rm W}\left(1+\frac{\mu\Lambda'}{2i}\right)\hat{\rho}'_{\rm W}(t') - \hat{\rho}'_{\rm W}(t')\left(1+\frac{\mu\Lambda'}{2i}\right)\hat{H}'_{\rm W}\right] \ . \tag{12}$$

Equation (12), when expressed in unscaled units, is the mixed quantum–classical Liouville equation (Eq. 1). The expansion of the evolution operator, expressed in scaled units, is analytic in μ. By contrast, the development of the unscaled form of the evolution operator in powers of $\hbar$ is not analytic owing to the factor of $1/\hbar$ multiplying the commutator in Eq. (6).

Equation (12) leads to the introduction of the quantum–classical bracket and Liouville operator,

$$(\hat{H}'_{\rm W}, \hat{A}'_{\rm W}) = i\mathscr{L}'\hat{A}'_{\rm W} = i\left[\hat{H}'_{\rm W}\left(1+\frac{\mu\Lambda'}{2i}\right)\hat{A}'_{\rm W} - \hat{A}'_{\rm W}\left(1+\frac{\mu\Lambda'}{2i}\right)\hat{H}'_{\rm W}\right] \ , \tag{13}$$

where the $\mathcal{O}(\mu)$ dependence is manifest. Using these scaled units, the action of the mixed quantum–classical Liouville operator on the product of two operators, $\hat{C}'_{\rm W} = \hat{A}'_{\rm W}(1+\mu\Lambda'/2i)\hat{B}'_{\rm W}$ is

$$i\hat{\mathscr{L}}'\hat{C}'_{\rm W} = (i\hat{\mathscr{L}}'\hat{A}'_{\rm W})\left(1+\frac{\mu\Lambda'}{2i}\right)\hat{B}'_{\rm W} + \hat{A}'_{\rm W}\left(1+\frac{\mu\Lambda'}{2i}\right)(i\hat{\mathscr{L}}'\hat{B}'_{\rm W}) + \mathcal{O}(\mu^2) \ . \tag{14}$$

Given this result we find that [19]

$$\hat{C}'_{\rm W}(t') = {\rm e}^{i\hat{\mathscr{L}}'t'}\hat{C}'_{\rm W} = \left({\rm e}^{i\hat{\mathscr{L}}'t'}\hat{A}'_{\rm W}\right)\left(1+\frac{\mu\Lambda'}{2i}\right)\left({\rm e}^{i\hat{\mathscr{L}}'t'}\hat{B}'_{\rm W}\right) + \mathcal{O}(\mu^2) = \hat{A}'_{\rm W}(t')\left(1+\frac{\mu\Lambda'}{2i}\right)\hat{B}'_{\rm W}(t') + \mathcal{O}(\mu^2) \ . \tag{15}$$

Therefore, the quantum–classical evolution of a composite operator cannot be determined exactly in terms of the quantum–classical evolution of its constituent operators, but only to terms $\mathcal{O}(\mu^2)$, in contrast both to quantum and to classical dynamics.

Furthermore, given three arbitrary operators, the Jacobi relation holds only to linear order in the small parameter μ [19, 25],

$$\left[\hat{A}'_{\rm W}, (\hat{B}'_{\rm W}, \hat{C}'_{\rm W})\right] + \left[\hat{C}'_{\rm W}, (\hat{A}'_{\rm W}, \hat{B}'_{\rm W})\right] + \left[\hat{B}'_{\rm W}, (\hat{C}'_{\rm W}, \hat{A}'_{\rm W})\right] = \mathcal{O}(\mu^2) \ , \tag{16}$$

for quantum–classical algebra.

These results have implications for the evaluation of transport properties and time correlation functions in quantum–classical dynamics [19, 25].

3 Representation in basis sets

The formal solutions of Eqs. (1) and (2) are

$$\hat{\rho}_{\rm W}(R,P,t) = {\rm e}^{-i\hat{\mathscr{L}}t}\hat{\rho}_{\rm W}(R,P,0),$$
$$\hat{A}_{\rm W}(R,P,t) = {\rm e}^{i\hat{\mathscr{L}}t}\hat{A}_{\rm W}(R,P,0) \ , \tag{17}$$

since the quantum–classical Liouville operator is time-independent if the Hamiltonian is independent of time. The density matrix and observable are abstract operators in the Hilbert space of the quantum subsystem and these equations may be expressed in any convenient basis to obtain their solution. Letting $\{|\alpha\rangle\}$ be a set of basis vectors that spans the Hilbert space of the quantum subsystem, Eq. (17) may be written as

$$A^{\alpha\alpha'}_{\rm W}(R,P,t) = \sum_{\beta\beta'}\left({\rm e}^{i\hat{\mathscr{L}}t}\right)_{\alpha\alpha',\beta\beta'} A^{\beta\beta'}_{\rm W}(R,P,0) \ , \tag{18}$$

where $A^{\alpha\alpha'}_{\rm W}(R,P,t) = \langle\alpha|\hat{A}_{\rm W}(R,P,t)|\alpha'\rangle$. The nature of the problem being investigated will often dictate the most convenient choice of basis to be used in the calculation. Two especially useful quantum bases in which to represent the dynamics are the subsystem basis and the adiabatic basis.

3.1 Subsystem basis

Writing the Hamiltonian as

$$\hat{H}_{\rm W}(R,P) = H_{\rm b}(R,P) + \hat{H}_{\rm s} + \hat{V}_{\rm c}(\hat{q},R) \ , \tag{19}$$

the subsystem basis is given by the solutions of the eigenvalue problem, $\hat{H}_{\rm s}|\alpha\rangle = \epsilon_\alpha|\alpha\rangle$. In this basis the Liouville operator takes the form [17]

$$i\mathscr{L}_{\alpha\alpha',\beta\beta'} = (i\tilde{\omega}_{\alpha\alpha'} + iL_{\rm b})\delta_{\alpha\beta}\delta_{\alpha'\beta'} + \delta_{\alpha\beta}\left(-\frac{i}{\hbar}V_{\rm c}^{\beta'\alpha'} - \frac{1}{2}\frac{\partial V_{\rm c}^{\beta'\alpha'}}{\partial R}\cdot\frac{\partial}{\partial P}\right) + \delta_{\alpha'\beta'}\left(\frac{i}{\hbar}V_{\rm c}^{\alpha\beta} - \frac{1}{2}\frac{\partial V_{\rm c}^{\alpha\beta}}{\partial R}\cdot\frac{\partial}{\partial P}\right) \ , \tag{20}$$

where $\tilde{\omega}_{\alpha\alpha'} = (\epsilon_\alpha - \epsilon_{\alpha'})/\hbar$, $V_c^{\alpha\alpha'} = \langle\alpha|\hat{V}_c|\alpha'\rangle$ and the bath Liouville operator is $iL_b = \left[\frac{P}{M}\frac{\partial}{\partial R} + F_b(R)\frac{\partial}{\partial P}\right]$ with $F_b(R) = -\partial V_b/\partial R$ the force on the bath particles.

3.2 Adiabatic basis

The adiabatic basis vectors, $|\alpha;R\rangle$, are given by the solutions of $\hat{h}_W|\alpha;R\rangle = E_\alpha(R)|\alpha;R\rangle$, where $\hat{h}_W = \frac{\hat{p}^2}{2m} + \hat{V}_W(\hat{q},R)$. We adopt an Eulerian view of the dynamics so that the adiabatic basis vectors are parameterized by the time-independent values of the bath coordinates R. The Liouville operator has matrix elements, [17]

$$\begin{aligned} i\mathscr{L}_{\alpha\alpha',\beta\beta'} &= (i\omega_{\alpha\alpha'} + iL_{\alpha\alpha'})\delta_{\alpha\beta}\delta_{\alpha'\beta'} - J_{\alpha\alpha',\beta\beta'} \\ &\equiv i\mathscr{L}^0_{\alpha\alpha'}\delta_{\alpha\beta}\delta_{\alpha'\beta'} - J_{\alpha\alpha',\beta\beta'} \ , \end{aligned} \tag{21}$$

where $\omega_{\alpha\alpha'}(R) = [E_\alpha(R) - E_{\alpha'}(R)]/\hbar$ is a frequency determined by the difference in energies of adiabatic states and $iL_{\alpha\alpha'}$ is the Liouville operator that describes classical evolution determined by the mean of the Hellmann–Feynman forces for adiabatic states α and α',

$$iL_{\alpha\alpha'} = \frac{P}{M}\cdot\frac{\partial}{\partial R} + \frac{1}{2}\left(F_W^\alpha + F_W^{\alpha'}\right)\cdot\frac{\partial}{\partial P} \ . \tag{22}$$

The operator $J_{\alpha\alpha',\beta\beta'}$ is responsible for nonadiabatic transitions and corresponding variations of the bath momentum, and has the form

$$\begin{aligned} J_{\alpha\alpha',\beta\beta'} = &-\frac{P}{M}\cdot d_{\alpha\beta}\left(1 + \frac{1}{2}S_{\alpha\beta}\cdot\frac{\partial}{\partial P}\right)\delta_{\alpha'\beta'} \\ &-\frac{P}{M}\cdot d^*_{\alpha'\beta'}\left(1 + \frac{1}{2}S^*_{\alpha'\beta'}\cdot\frac{\partial}{\partial P}\right)\delta_{\alpha\beta} \ , \end{aligned} \tag{23}$$

where $d_{\alpha\beta} = \langle\alpha;R|\nabla_R|\beta;R\rangle$ is the nonadiabatic coupling matrix element, $S_{\alpha\beta} = \Delta E_{\alpha\beta}\hat{\boldsymbol{d}}_{\alpha\beta}(\frac{P}{M}\cdot\hat{\boldsymbol{d}}_{\alpha\beta})^{-1}$ with $\Delta E_{\alpha\beta}(R) = E_\alpha(R) - E_\beta(R)$.

Since the quantum–classical evolution equation is independent of the basis, we see that its solution can be constructed using any convenient basis. In contrast, quantum–classical equations of motion have been constructed by first representing the partially Wigner transformed quantum equations of motion in a basis and then making approximations to yield a quantum–classical limit [26, 27]. However, this approach may lead to equations that do not conserve the energy and are naturally basis-set dependent.

4 Solution of evolution equations

The representation in the adiabatic basis is especially instructive for formulating the dynamics in terms of surface-hopping trajectories [17, 28]. To this end the evolution operator may be separated into diagonal and off-diagonal parts as in Eq. (21) and this decomposition substituted into the operator identity,

$$e^{(\hat{A}+\hat{B})t} = e^{\hat{A}t} + \int_0^t dt'\, e^{\hat{A}(t-t')}\hat{B}e^{(\hat{A}+\hat{B})t'} \ , \tag{24}$$

to obtain

$$\begin{aligned} \left(e^{-i\hat{\mathscr{L}}t}\right)_{\alpha\alpha',\beta\beta'} = &\, e^{-i\mathscr{L}^0_{\alpha\alpha'}t}\delta_{\alpha\beta}\delta_{\alpha'\beta'} + \sum_{\nu\nu'}\int_0^t dt'\, e^{-i\mathscr{L}^0_{\alpha\alpha'}(t-t')} \\ &\times J_{\alpha\alpha'\nu\nu'}\left(e^{-i\hat{\mathscr{L}}t'}\right)_{\nu\nu',\beta\beta'} \ . \end{aligned} \tag{25}$$

This equation gives the evolution operator as an integral equation in Dyson form. The diagonal part of the quantum–classical evolution superoperator, $\exp\{i\mathscr{L}^0_{\alpha\alpha'}t\}$, may be written explicitly in terms of classical evolution on the $(\alpha\alpha')$ surface as

$$\begin{aligned} e^{-i\mathscr{L}^0_{\alpha\alpha'}(t-t')} &= e^{-i\int_t^{t'} d\tau\, \omega_{\alpha\alpha'}(R_{\alpha\alpha',\tau})}e^{-iL_{\alpha\alpha'}(t-t')} \\ &\equiv \mathscr{W}_{\alpha\alpha'}(t,t')e^{-iL_{\alpha\alpha'}(t-t')} \ , \end{aligned} \tag{26}$$

as demonstrated in Ref. [17], thus, it involves the product of a phase factor and a classical evolution operator. If $\alpha = \alpha'$ the phase factor is unity and evolution is by Newton's equations of motion on a single α adiabatic surface.

The solution of the integral equation (Eq. 25) may be found by iteration to yield a representation of the dynamics as a sequence of terms involving increasing numbers of nonadiabatic transitions [17],

$$\begin{aligned} \rho_W^{\alpha_0\alpha'_0}(R,P,t) = &\, e^{-i\mathscr{L}^0_{\alpha_0\alpha'_0}t}\rho_W^{\alpha_0\alpha'_0}(R,P) + \sum_{n=1}^{\infty} \\ &\times \sum_{(\alpha_1\alpha'_1)\ldots(\alpha_n\alpha'_n)}\int_0^{t_0} dt_1\int_0^{t_1} dt_2 \ldots \int_0^{t_{n-1}} dt_n \\ &\times \prod_{k=1}^{n}\left[e^{-i\mathscr{L}^0_{\alpha_{k-1}\alpha'_{k-1}}(t_{k-1}-t_k)}J_{\alpha_{k-1}\alpha'_{k-1},\alpha_k\alpha'_k}\right] \\ &\times e^{-i\mathscr{L}^0_{\alpha_n\alpha'_n}t_n}\rho_W^{\alpha_n\alpha'_n}(R,P) \ , \end{aligned} \tag{27}$$

where $\rho_W^{\alpha\alpha'}(R,P)$ is the initial value of the density matrix element.

The successive terms in the series correspond to increasing numbers of nonadiabatic transitions, starting with the first term that describes simple adiabatic dynamics. As an example of the structure of the terms in the series, consider computing populations given by the diagonal elements of the density matrix. The quantum–classical approximation to the population in state α at phase point (R,P) at time t is given by a sum of terms starting with adiabatic evolution on state α. The contributions to $\rho_W^{\alpha\alpha}(R,P,t)$ are determined by backward evolution from time t to time 0. Single nonadiabatic contributions appear next where transitions to states β $(\beta \neq \alpha)$ occur at times t' intermediate between t and 0. Such transitions are accompanied by continuous momentum changes in the environment specified by the term in J involving a momentum derivative. Since a single quantum transition takes place this contribution to $\rho_W^{\alpha\alpha}(R,P,t)$ must arise from an off-diagonal density matrix element, $\rho_W^{\alpha\beta}$ at time 0. During the portion of the evolution segment from t' to 0, the classical environmental phase

space coordinates are propagated on the mean of the two α and β adiabatic surfaces and a phase factor, $\mathscr{W}_{\alpha\beta}$, contributes to the population in state α.

Similar interpretations can be given to the higher-order terms in the series involving multiple nonadiabatic transitions. For example, if the initial state is diagonal, then only contributions with even numbers of nonadiabatic transitions can affect the populations at time t. In this case, as a consequence of the presence of the phase factor $\mathscr{W}$, between any two nonadiabatic transitions the system is in a coherent superposition of states, which is destroyed by the final nonadiabatic transition. A schematic example of a trajectory with two nonadiabatic transitions is shown in Fig. 1.

Instead of evolving the density matrix, we may consider the time evolution of an operator $\hat{A}_{\mathrm{W}}(R,P)$ and compute its expectation value at time t as

$$\begin{aligned}\langle A\rangle(t) &= \sum_{\alpha_0\alpha_0'}\int \mathrm{d}R\,\mathrm{d}P\,A_{\mathrm{W}}^{\alpha_0\alpha_0'}(R,P)\rho_{\mathrm{W}}^{\alpha_0'\alpha_0}(R,P,t)\\ &= \sum_{\alpha_0\alpha_0'}\int \mathrm{d}R\,\mathrm{d}P\,A_{\mathrm{W}}^{\alpha_0\alpha_0'}(R,P,t)\rho_{\mathrm{W}}^{\alpha_0'\alpha_0}(R,P)\ , \end{aligned}\tag{28}$$

where

$$\begin{aligned}A_{\mathrm{W}}^{\alpha_0\alpha_0'}(R,P,t) &= \mathrm{e}^{i\mathscr{L}^0_{\alpha_0\alpha_0'}t}A_{\mathrm{W}}^{\alpha_0\alpha_0'}(R,P)\\ &\quad+\sum_{n=1}^{\infty}(-1)^n\sum_{(\alpha_1\alpha_1')\ldots(\alpha_n\alpha_n')}\int_0^{t_0}\mathrm{d}t_1\int_0^{t_1}\mathrm{d}t_2\ldots\int_0^{t_{n-1}}\mathrm{d}t_n\\ &\quad\times\prod_{k=1}^{n}\left[\mathrm{e}^{i\mathscr{L}^0_{\alpha_{k-1}\alpha_{k-1}'}(t_{k-1}-t_k)}J_{\alpha_{k-1}\alpha_{k-1}',\alpha_k\alpha_k'}\right]\\ &\quad\times\mathrm{e}^{i\mathscr{L}^0_{\alpha_n\alpha_n't_n}}A_{\mathrm{W}}^{\alpha_n\alpha_n'}(R,P)\ . \end{aligned}\tag{29}$$

Equation (29) is computationally much more convenient than Eq. (27) for the evaluation of expectation values since one may use the initial density as a weight to sample the phase space points in the average (Eq. 28).

5 The operator J

The operator J is responsible for nonadiabatic transitions and concomitant momentum changes in the bath.

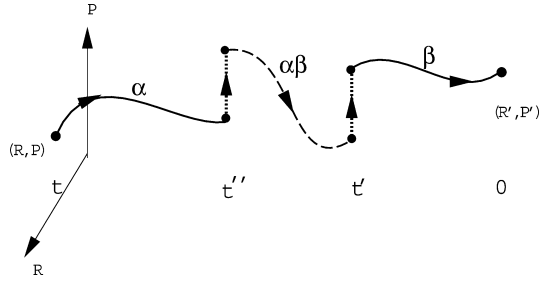

Fig. 1. A trajectory segment with two nonadiabatic transitions that contributes to the diagonal element $\rho_{\mathrm{W}}^{\alpha\alpha}(R,P,t)$ arising from $\rho_{\mathrm{W}}^{\beta\beta}(R,P,t=0)$. In the time segment between t'' and t' the system evolves coherently and contains the phase factor $\mathscr{W}_{\alpha\beta}$

It appears in exponential form in the evolution operator $\mathrm{e}^{i\hat{\mathscr{L}}t}$ or directly in the iterated Dyson integral equation form of the solution in Eqs. (27) and (29). The manner in which this operator is implemented in numerical simulations is one of the essential and most challenging aspects of the construction of algorithms for quantum–classical surface-hopping dynamics. Later we shall discuss two ways of accounting for the action of this operator on functions of the bath momentum in the context of the iterated Dyson form of surface-hopping dynamics. Subsequently, we comment on other schemes that are under development in improved algorithms for the evolution.

5.1 Finite difference approximation

From the form of J given in Eq. (23), one can see that it involves bath momentum derivatives of the form $S_{\alpha\beta}\cdot\nabla_P = \Delta E_{\alpha\beta}(\frac{P}{M}\cdot\hat{\boldsymbol{d}}_{\alpha\beta})^{-1}\hat{\boldsymbol{d}}_{\alpha\beta}\cdot\nabla_P$. Consequently, momentum derivatives along the nonadiabatic coupling vectors must be evaluated. One way to evaluate such derivatives is by a straightforward finite difference scheme where

$$\hat{\boldsymbol{d}}_{\alpha\beta}\cdot\nabla_P f(P) \approx (\Delta_P)^{-1}[f(P+\hat{\boldsymbol{d}}_{\alpha\beta}\Delta_P)-f(P)]\ ,\tag{30}$$

where Δ_P is a small scalar displacement. As a result, in this scheme, every time a momentum derivative acts the classical trajectory branches and a pair of trajectories must be followed until the next nonadiabatic transition where a similar branching occurs. Thus a realization of the dynamics with n nonadiabatic transitions involves 2^n trajectories. This simplistic algorithm has been used to illustrate the properties of exact quantum–classical surface-hopping dynamics for model systems [28]. In practice it is useful only for short-time computations involving small numbers of nonadiabatic transitions, as we shall show in the next section.

5.2 Momentum-jump approximation

Branching of trajectories may be avoided by making a "momentum-jump" approximation to J that converts this operator into a momentum translation operator whose effect on any function of the momentum is to shift the momentum by some value [3, 17]. The momentum-jump approximation to J may be constructed in the following way. We saw that the operator J involves differential operators of the form $\left[1+\frac{1}{2}S_{\alpha\beta}(P)\cdot\frac{\partial}{\partial P}\right]$ acting on functions of the classical phase space coordinates. Before making this approximation, it is first convenient to make use of the explicit form $S_{\alpha\beta}=\Delta E_{\alpha\beta}\hat{\boldsymbol{d}}_{\alpha\beta}(\frac{P}{M}\cdot\hat{\boldsymbol{d}}_{\alpha\beta})^{-1}$ and introduce a change of variables to write the operator in the form

$$\left(1+\frac{1}{2}S_{\alpha\beta}\cdot\frac{\partial}{\partial P}\right)=1+\Delta E_{\alpha\beta}M\frac{\partial}{\partial(P\cdot\hat{\boldsymbol{d}}_{\alpha\beta})^2}\ .\tag{31}$$

Now the prefactor of the (modified) momentum derivative depends only on the configuration and not on the momentum.

The action of the operator on any function $f(P)$ of the momentum may be written approximately as

$$\left(1+\Delta E_{\alpha\beta}M\frac{\partial}{\partial(P\cdot\hat{d}_{\alpha\beta})^2}\right)f(P)$$
$$\approx \mathrm{e}^{\Delta E_{\alpha\beta}M\partial/\partial(P\cdot\hat{d}_{\alpha\beta})^2}f(P)=f\Big[\hat{d}^{\perp}_{\alpha\beta}(P\cdot\hat{d}^{\perp}_{\alpha\beta})$$
$$+\hat{d}_{\alpha\beta}\mathrm{sgn}(P\cdot\hat{d}_{\alpha\beta})\sqrt{(P\cdot\hat{d}_{\alpha\beta})^2+\Delta E_{\alpha\beta}M}\Big]\ . \qquad (32)$$

In the second approximate equality on the right-hand side of this equation we have approximated the sum by an exponential. The momentum vector may be written in terms of its components along $\hat{d}_{\alpha\beta}$ and a perpendicular vector $\hat{d}^{\perp}_{\alpha\beta}$, $P=\hat{d}_{\alpha\beta}(\hat{d}_{\alpha\beta}\cdot P)+\hat{d}^{\perp}_{\alpha\beta}(\hat{d}^{\perp}_{\alpha\beta}\cdot P)$. In the last line, we used the fact that the exponential operator is a translation operator in the variable $(P\cdot\hat{d}_{\alpha\beta})^2$. If the energy difference times the mass $\Delta E_{\alpha\beta}$ is small compared to twice the bath kinetic energy corresponding to the momentum along $\hat{d}_{\alpha\beta}$, $(P\cdot\hat{d}_{\alpha\beta})^2/M$, we may expand the square root in the argument of f to obtain

$$f\Big[\hat{d}^{\perp}_{\alpha\beta}(P\cdot\hat{d}^{\perp}_{\alpha\beta})+\hat{d}_{\alpha\beta}\mathrm{sgn}(P\cdot\hat{d}_{\alpha\beta})\sqrt{(P\cdot\hat{d}_{\alpha\beta})^2+\Delta E_{\alpha\beta}M}\Big]$$
$$\approx f\Big(P+\frac{1}{2}S_{\alpha\beta}\Big)\ . \qquad (33)$$

Thus, to lowest order in the small parameter $\Delta E_{\alpha\beta}M/(P\cdot\hat{d}_{\alpha\beta})^2$ we may write the operators in J as momentum translation (jump) operators.

A few observations concerning the nature of the momentum-jump approximation can be made on the basis of these equations. If $\Delta E_{\alpha\beta}<0$ (an upward transition from $\alpha\to\beta$) and $(P\cdot\hat{d}_{\alpha\beta})^2/M<|\Delta E_{\alpha\beta}|$ so that there is insufficient kinetic energy for bath momenta along $\hat{d}_{\alpha\beta}$ for the quantum transition to occur, the argument of the square root is negative leading to imaginary momentum changes. In addition, if $\Delta E_{\alpha\beta}M/(P\cdot\hat{d}_{\alpha\beta})^2>1$ the conditions for the validity of the momentum-jump approximation are violated. In both cases the $P\cdot\hat{d}_{\alpha\beta}$ prefactor in the expression for J will make the contribution small, providing motivation for discarding these trajectories.

It is interesting to observe that momentum jumps in the environment corresponding to $S_{\alpha\beta}$ are associated with quantum transitions $\alpha\to\beta$ between adiabatic states in Tully's surface-hopping algorithm [2].

In the following section we provide some illustrations of the simulation of quantum–classical surface-hopping dynamics using the schemes outlined previously.

6 Simulations of nonadiabatic dynamics

While the quantum–classical formalism discussed earlier is applicable to any quantum system coupled to any classical environment, it is instructive to apply the simulation methods to simple spin-boson models [29, 30]. Such models often not only capture the essential physics or chemistry of many real systems but also have the advantage that numerically exact results are available for comparisons [31]. Furthermore, for this model quantum–classical dynamics is exact, so one may test directly the efficacy of different algorithms without concerns related to the validity of the quantum–classical approximation to the full quantum dynamics [32].

The spin-boson Hamiltonian describes a two-level system with states $\{|\uparrow>,|\downarrow>\}$ bilinearly coupled to a bath of N_{B} harmonic oscillators with masses M_j and frequencies ω_j. The Hamiltonian is

$$\hat{H}=-\hbar\Omega\hat{\sigma}_x+\sum_{j=1}^{N_{\mathrm{B}}}\left(\frac{\hat{P}_j^{\,2}}{2M_j}+\frac{1}{2}M_j\omega_j^2\hat{Q}_j^2-c_j\hat{Q}_j\hat{\sigma}_z\right)\ , \qquad (34)$$

where $2\hbar\Omega$ is the energy gap of the isolated two-state system and σ_x and σ_z are Pauli spin matrices. The coupling constants c_j and frequencies ω_j are given by [31] $c_j=\sqrt{\xi\hbar\omega_0M_j}\omega_j$ with $\omega_j=-\omega_{\mathrm{c}}\ln\Big(1-j\frac{\omega_0}{\omega_{\mathrm{c}}}\Big)$ and $\omega_0=\frac{\omega_{\mathrm{c}}}{N_{\mathrm{B}}}\big(1-\mathrm{e}^{-\omega_{\max}/\omega_{\mathrm{c}}}\big)$, corresponding to a system with ohmic spectral density characterized by the Kondo parameter ξ and frequency ω_{c}. The parameter $\omega_{\max}$ is a cutoff frequency.

The quantum–classical formalism requires the partial Wigner transform of this quantum Hamiltonian over the bath degrees of freedom. Carrying out this transformation we obtain

$$\hat{H}_{\mathrm{W}}=-\hbar\Omega\hat{\sigma}_x+\sum_{j=1}^{N_{\mathrm{B}}}\left(\frac{P_j^{\,2}}{2M_j}+\frac{1}{2}M_j\omega_j^2R_j^2-c_jR_j\hat{\sigma}_z\right)\ . \qquad (35)$$

which depends on the classical phase space coordinates (R,P) and the spin degrees of freedom.

6.1 Dyson integral equation

The series solution for the mean value of a dynamical variable in Eqs. (28) and (29) may be evaluated by a hybrid Monte Carlo–molecular dynamics scheme where the phase space point, the quantum transitions and the times at which they occur are sampled from suitable distributions [17, 28, 32].

First, we consider a method to evaluate the series term by term. This scheme, while only appropriate if the dynamics of interest involves a small number of nonadiabatic transitions, has the advantage that one may analyze in detail how the various terms contribute to the average value. The term-by-term calculation of the Dyson expansion for $\langle A\rangle(t)$ requires that, for a fixed number n of quantum transitions, one must sample the times $\tau_1,\ldots,\tau_n$ at which the transitions occur. If we let $\tau_0=0$, then for $i=1,\ldots,n$, τ_i may be sampled within the interval (t,τ_{i-1}) with probability $(t-\tau_{i-1})^{-1}$. The operator J acts at each time τ_i. As discussed earlier, the Dyson expansion results from the sum/integral over all possible values of τ_i, $i=1,\ldots,n$, of $n+1$ classical-like trajectory segments resulting from adiabatic evolution on potential energy surfaces characterized by the pair of

indices $(\alpha_i\alpha_i')$, interspersed by n quantum transitions. According to Eq. (26) the ith trajectory segment carries a quantum phase factor $\mathscr{W}_{\alpha_i\alpha_i'}$ which is, of course, unity if $\alpha_i = \alpha_i'$.

Since J is composed of two terms (see Eq. 23), when a transition occurs at time τ_i, the way it acts can be treated stochastically and one may sample with probability $1/2$ to determine which of the two terms acts. If the initial state is labelled $(\beta\beta')$, the first term of J changes the β index while the second term changes the β' index. If the Hilbert space is completely spanned by a number, s, of states, the initial state can be transformed by the action of J into any of the other $s-1$ states. One can associate a statistical weight w_s, to each state and use this weight to determine which specific transition, out of the allowed $s-1$ transitions, occurs. For example, consider a system with $s=3$ states with associated weights w_s, $s=1,2,3$. Imagine that at a certain τ_i along the evolution the system is in the state $(\alpha_i,\alpha_i') = (1,1)$ and the random sampling has determined that the first term in the J term must act. Then a transition $\alpha_i = 1 \rightarrow \alpha_{i-1}$ can occur with $\alpha_{i-1} = 2$ or 3 with probabilities w_2 and w_3, respectively. These probabilities can be used to determine if one must apply $J_{21,11}$ or $J_{31,11}$. The $(P/M)\cdot d_{\alpha_i\alpha_{i-1}}$ factor must be computed and stored to determine the final overall weight of the trajectory to the Dyson expansion. As previously discussed, in the momentum-jump approximation, a transition can be rejected if there is insufficient kinetic energy for it to take place or if the momentum shift is too high.

Results of calculations of the mean population difference in the spin up and down states, $\langle\sigma_z\rangle(t)$, are shown in Fig. 2. This figure plots the individual contributions to $\langle\sigma_z\rangle(t)$ coming from adiabatic dynamics and nonadiabatic dynamics with $n=1,2,3$ and 4 jumps. From these results one can see that in the time interval shown the successive contributions decrease in magnitude, indicating convergence of the series for $\langle\sigma_z\rangle(t)$. For longer times successively more terms in the series corresponding to greater numbers of nonadiabatic transitions must be taken into account.

The sum of the adiabatic and the first four nonadiabatic contributions in the Dyson series for $\langle\sigma_z\rangle(t)$ is compared in Fig. 3 with the corresponding result obtained using a finite-difference evaluation of the momentum derivative in J. One can see that the finite-difference and momentum-jump approximations are in good accord for our spin-boson model. For longer times where higher-order terms in the series must be taken into account, the solution becomes numerically unstable and this method cannot be used to obtain these terms in the series.

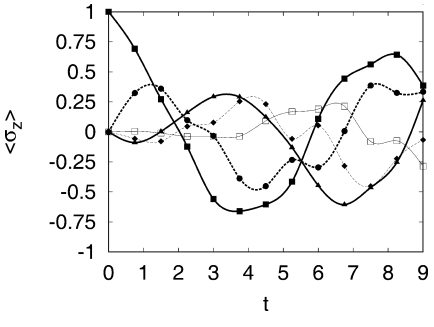

Fig. 2. Adiabatic and nonadiabatic contributions to the average population difference between the spin up and spin down states, $\langle\sigma_z\rangle(t)$, versus time. System parameters $\xi = 0.1$, $\beta = 3.0/\hbar\omega_c$, $N_B = 10$, $\omega_{max} = 3.0$ and $\Omega = \omega_c/3$. Different curves correspond to contributions in the Dyson series for $n = 0,\ldots,4$: $n=0$ adiabatic dynamics (*filled squares*); $n=1$ (*circles*); $n=2$ (*triangles*); $n=3$ (*diamonds*); $n=4$ (*open squares*)

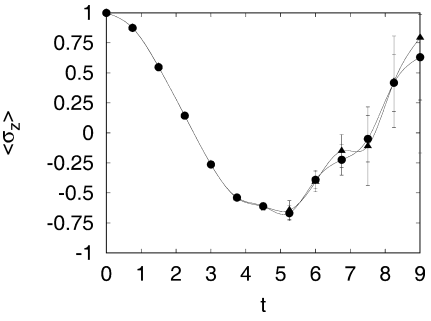

Fig. 3. Comparison of momentum-jump and finite-difference approximations to the J operator in the calculation of $\langle\sigma_z\rangle(t)$ including up to four nonadiabatic transitions. The system parameters are the same as in Fig. 2. Momentum-jump approximation (*circles*); finite-difference approximation using $\Delta_P = 0.05$ (triangles)

6.2 Sequential short-time propagation

The previous scheme, while conceptually attractive, does not provide the most efficient way to simulate quantum–classical dynamics since each time t requires a separate calculation. It is a simple matter to construct a scheme that allows one to obtain the entire history in a single simulation. This method relies on writing the quantum–classical time evolution operator as a sequence of small finite-time intervals and then concatenating the results to obtain the solution.

Since the quantum–classical Liouville operator $\hat{\mathscr{L}}$ is time-independent, the evolution operator may be written as a composition of evolution operators in time segments of arbitrary length [33]. Suppose we divide the time interval t into N segments of lengths $\Delta t_j = t_j - t_{j-1}$. Then

$$\left(\mathrm{e}^{i\mathscr{L}t}\right)_{\alpha_0\alpha_0',\alpha_N\alpha_N'} = \sum_{(\alpha_1\alpha_1')\ldots(\alpha_{N-1}\alpha_{N-1}')} \times \prod_{j=1}^{N}\left(\mathrm{e}^{i\mathscr{L}(t_j-t_{j-1})}\right)_{\alpha_{j-1}\alpha_{j-1}',\alpha_j\alpha_j'} . \tag{36}$$

If the time interval Δt is assumed to be sufficiently small, we can make a one-point approximation to the time integral by choosing a point t' in Δt. Letting $t' = t_j$ we obtain,

$$\begin{aligned}\left(\mathrm{e}^{i\hat{\mathscr{L}}(t_j-t_{j-1})}\right)_{\alpha_{j-1}\alpha_{j-1}',\alpha_j\alpha_j'} &\approx \mathrm{e}^{i\mathscr{L}^0_{\alpha_{j-1}\alpha_{j-1}'}(t_j-t_{j-1})} \\ &\times\left(\delta_{\alpha_{j-1}\alpha_j}\delta_{\alpha_{j-1}'\alpha_j'} - \Delta t J_{\alpha_{j-1}\alpha_{j-1}',\alpha_j\alpha_j'}\right) \\ &= \mathscr{W}_{\alpha_{j-1}\alpha_{j-1}'}(t_{j-1},t_j)\mathrm{e}^{iL_{\alpha_{j-1}\alpha_{j-1}'}(t_j-t_{j-1})} \\ &\times\left(\delta_{\alpha_{j-1}\alpha_j}\delta_{\alpha_{j-1}'\alpha_j'} - \Delta t J_{\alpha_{j-1}\alpha_{j-1}',\alpha_j\alpha_j'}\right) .\end{aligned} \tag{37}$$

At the end of each small segment, the system either may remain in the same pair of adiabatic states or may make a transition to a new pair of states. Substituting this expression into Eq. (36) we obtain

$$\left(\mathrm{e}^{i\mathscr{L}t}\right)_{\alpha_0\alpha'_0,\alpha_N\alpha'_N} \approx \sum_{(\alpha_1\alpha'_1)(\alpha_2\alpha'_2)\ldots(\alpha_{N-1}\alpha'_{N-1})} \times \prod_{j=1}^{N} \mathrm{e}^{i\mathscr{L}^0_{\alpha_{j-1}\alpha'_{j-1}}(t_j - t_{j-1})} \times \left(\delta_{\alpha_{j-1}\alpha_j}\delta_{\alpha'_{j-1}\alpha'_j} - \Delta t J_{\alpha_{j-1}\alpha'_{j-1},\alpha_j\alpha'_j}\right) \quad . \tag{38}$$

Here and later $t_j = j\Delta t$ and $t_N = t$. In the limit $N \to \infty$, $\Delta t \to 0$ with $N\Delta t = t$ we recover the iterated form of the Dyson integral propagator. This may be seen by expanding the terms in Eq. (38) and using the propagator to compute $A_{\mathrm{W}}^{\alpha_0\alpha'_0}(R,P,t)$ to obtain

$$\begin{aligned} A_{\mathrm{W}}^{\alpha_0\alpha'_0}(R,P,t) = {} & \mathrm{e}^{i\mathscr{L}^0_{\alpha_0\alpha'_0}t} A_{\mathrm{W}}^{\alpha_0\alpha'_0}(R,P) \\ & + \sum_{n=1}^{N}(-1)^n \sum_{(\alpha_1\alpha'_1)\ldots(\alpha_{n-1}\alpha'_{n-1})} \\ & \times \sum_{k_1=1}^{N-n+1} \sum_{k_2=k_1+1}^{N-n+2} \cdots \sum_{k_n=k_{n-1}+1}^{N} \mathrm{e}^{i\mathscr{L}^0_{\alpha_0\alpha'_0}(t_{k_1}-t_0)} \\ & \times (\Delta t J_{\alpha_0\alpha'_0,\alpha_1\alpha'_1}) \mathrm{e}^{i\mathscr{L}^0_{\alpha_1\alpha'_1}(t_{k_2}-t_{k_1})} \\ & \times (\Delta t J_{\alpha_1\alpha'_1,\alpha_2\alpha'_2}) \cdots (\Delta t J_{\alpha_{n-1}\alpha'_{n-1},\alpha_N\alpha'_N}) \\ & \times \mathrm{e}^{i\mathscr{L}^0_{\alpha_N\alpha'_N}(t-t_{kn})} A_{\mathrm{W}}^{\alpha_N\alpha'_N}(R,P) \quad . \end{aligned} \tag{39}$$

In this equation no sum over the $(\alpha_i\alpha'_i)$ indices is to be taken for $n = 1$. By inspection, it is evident that in the limit given previously, Eq. (39) is the discretized version of the iterated form of the Dyson expression in Eq. (29).

The implementation of the sequential short-time propagation algorithm is considerably simpler than that used for the term-by-term calculation of the Dyson series. The total time t of the calculation is divided into a fixed number of time slices. The most natural choice is to take the molecular dynamics integration time step Δt as the length of the slice. Using this choice, the phase space coordinates are propagated adiabatically for a single time step and the phase factor $\mathscr{W}$ is calculated for this time step. At the end of each single time step the probabilities

$$\Pi = \left|\frac{P}{M}\cdot d\right|\Delta t\left(1 + \left|\frac{P}{M}\cdot d\right|\Delta t\right)^{-1} \quad , \tag{40}$$

and $\Sigma = 1 - \Pi$, respectively, are used to accept or reject a quantum transition. If the transition is accepted a factor Π^{-1} is included in the observable and the operator $\Delta t J$ acts to change quantum state giving rise to another factor $\Delta t \frac{P}{M}\cdot d$ in the observable. If the transition is rejected the factor Σ^{-1} multiplies the observable. Ensemble averages can be calculated very efficiently for each single time step along the trajectory from a single calculation, while in the term-by-term method one needs a separate calculation for every t.

The scheme naturally permits the occurrence of a quantum transition at each time slice; however, there are limitations on the total time over which the simulation may be carried out. The realizations that contain a large number of nonadiabatic transitions involve oscillating phase factors associated with each adiabatic trajectory segment. In addition, each time J acts it provides a factor proportional to $\frac{P}{M}\cdot d$ which can oscillate in sign and magnitude. Consequently, large ensembles of such trajectories are needed to obtain good statistics. In practice, a trade-off is necessary to reduce the statistical error intrinsic in the calculation. To this aim one can set a bound, $n_{\max}$, on the allowed number of quantum transitions per trajectory so that the propagation of the trajectory is truncated at a time $t' \leq t$ when $n = n_{\max} + 1$. As a result the number of members in the ensemble can vary as a function of time. Because the number of allowed transitions is restricted to $n_{\max}$ the calculation will yield accurate results only for times t for which the dynamics is accurately represented by $n \leq n_{\max}$ nonadiabatic transitions.

The time evolution of $\langle\sigma_z\rangle(t)$ was computed using this algorithm and the results are compared with the numerically exact influence functional and the term-by-term Dyson method in Fig. 4. One can see that the results are in good accord. From the sequential short-time propagation algorithm, information at all intermediate times is available at a computational cost equivalent to that of a single point in the term-by-term method. For these spin-boson parameters ensembles of small numbers of trajectories are needed to obtain the results for $t \leq 9$. For example, ensembles of 10^4 trajectories or fewer reproduce the results shown in the figure. In the figure on can also see that beyond $t > 9$ numerical instabilities, which have their origin in the increasing magnitude of the product of weight factors Σ^{-1} and the errors introduced by the use of the momentum-jump approximation, become pronounced. Much larger ensembles whose sizes increase with time are needed to obtain reliable results.

It is of interest to extract additional information about the nonadiabatic dynamics from this calculation.

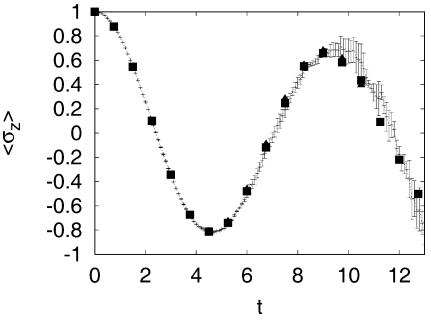

Fig. 4. Comparison of results for $\langle\sigma_z\rangle(t)$ using the Dyson series and sequential short-time propagation algorithms with influence functional results. System parameters $\xi = 0.007$, $\beta = 3.0/\hbar\omega_c$, $N = 10$, $\omega_{\max} = 3.0$ and $\Omega = \omega_c/3$. Dyson series (*squares*); sequential short-time propagation algorithm (*pluses with errorbars*); influence functional results (*triangles*). The triangles and squares overlap and are not always distinguishable in the graph

The average number of nonadiabatic transitions $\langle N_n \rangle(t)$ is plotted in Fig. 5 as a function of time. For up to intermediate times, this number grows linearly with time, indicating a constant mean transition probability per unit time of 0.204. For the longest times in this figure one observes deviations from linear behavior arising from the fact that the number of transitions was restricted to a maximum of $n_{\max} = 4$. Even for times up to $t = 9$ the deviations are not large, indicating that including up to four nonadiabatic transitions provides a good description of the dynamics.

It is possible to analyze the contributions of the individual nonadiabatic transitions in more detail by monitoring the fraction of trajectories, F_n, in the ensemble which undergo n transitions as a function of time. This fraction is plotted in Fig. 6 and it shows that indeed retaining up to four transitions captures the essential features of the dynamics in this time interval. Furthermore, as expected, the contributions from higher numbers of transitions have their major effects at progressively longer times: the $n = 0$ contribution peaks at $t = 0$, the $n = 1$ contribution at around $t = 5$, the $n = 2$ contribution at $t = 10$ and the $n = 3$ contribution at $t = 15$.

7 Conclusion

Quantum–classical evolution equations for either the density matrix or the dynamical variables provide a means to study the nonadiabatic dynamics of quantum systems embedded in general classical many-body environments. The evolution equations describe the coupled evolution of the quantum and classical subsystems and do not require a separate ansatz for the classical evolution segments, as is the case in other mixed quantum–classical schemes. The solutions of the evolution equations can be formulated in terms of surface-hopping dynamics which, in principle, can be carried out exactly in the context of quantum–classical dynamics. The results presented in this paper and the cited literature have demonstrated the utility of this scheme for studying nonadiabatic dynamics.

The construction of effective methods to simulate the evolution prescribed by the quantum–classical Liouville equation is a topic of current research. In addition to the methods discussed here, the quantum–classical evolution equations have been solved [34, 35] for low-dimensional models using the multiple-threads algorithm [36]. For some applications it is more convenient to work in the subsystem basis. The dynamics of the decay from excited states and simple barrier crossing problems have been investigated in this representation by associating Gaussian wave packets with the trajectory evolution [16].

Algorithms based on a Trotter factorization of the quantum–classical propagator are under development [27]. A Trotter factorization of the quantum–classical propagator in conjunction with Gaussian wavepacket evolution has been employed to obtain solutions to the quantum–classical Liouville equation [27]. Such schemes have the advantage that they avoid the use of the momentum-jump approximation and at the same time preserve the unitary character of the evolution.

One may also utilize algorithms based on stochastic quantum–classical evolution equations [37] where part of the classical bath is described by stochastic dynamics or reduced equations of motion where the classical bath variables are projected out of the description yielding equations for the quantum subsystem [38].

Although this paper has focused on simulation algorithms for quantum–classical dynamics and their interpretation in terms of surface-hopping trajectories, a statistical mechanical theory of quantum–classical dynamics has been developed [3, 19] which allows one to compute transport properties in terms of equilibrium time correlation functions. In particular, one may use this formalism to compute the rates of nonadiabatic chemical reactions directly from the reactive flux correlation functions [25].

While both the formalism for quantum-classical dynamics and the construction of efficient algorithms for its simulation are active areas of research that should see further development in the future, the results presented here show that the present approach to quantum dynamics already offers a promising route for the study of a variety problems in this area.

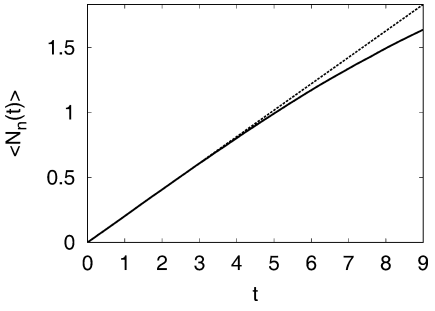

Fig. 5. Average number of nonadiabatic transitions $\langle N_n \rangle(t)$ versus time (*solid line*). The *dotted straight line* $\langle N_n \rangle(t) = 0.204\, t$ describes the ideal linear behavior corresponding to a constant mean transition probability per unit time

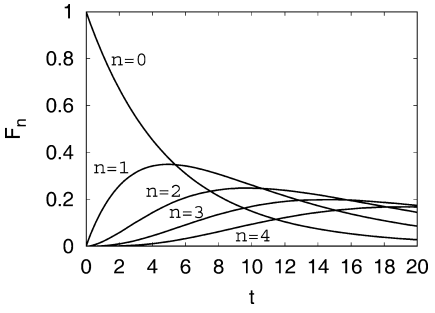

Fig. 6. The fraction of trajectories in the ensemble involving $n = 0$ (adiabatic dynamics with no transitions) and $n = 1, 2, 3$ and 4 nonadiabatic transitions versus time

Acknowledgements. This work was supported in part by a grant from the Natural Sciences and Engineering Research Council of Canada. Acknowledgement is made to the donors of The Petroleum Research Fund, administered by the ACS, for partial support

of this research. The visiting program of the Commissione Calcolo of INFM is acknowledged for supporting an extended visit of R.K. to Rome. D.M. acknowledges the support of Irish Higher Education Authority, through the PRTLI (cycle 3) IITAC program.

References

1. Herman MF (1994) Annu Rev Phys Chem 45: 83
2. Tully JC (1998) In: Thompson DL (ed). Modern methods for multidimensional dynamics computations in chemistry, World Scientific, New York, p 34
3. Kapral R, Ciccotti G (2003) In: Nielaba P, Mareschal M, Ciccotti G (eds) Bridging time scales: Molecular simulations for the next decade. SIMU Conference 2001. Springer, Berlin Heidelberg New York, p 445
4. (a) Pechukas P (1969) Phys Rev 181: 166; (b) Pechukas P (1969) Phys Rev 181: 174
5. Berendsen HJ, Mavri J (1993) J Phys Chem 97: 13464
6. Bala P, Lesyng B, McCammon JA (1994) Chem Phys Lett 219: 259
7. Egorov SA, Rabani E, Berne BJ (1999) J Chem Phys 110: 5238
8. (a) Tully JC (1990) J Chem Phys 93: 1061; (b) Tully JC (1991) Int J Quantum Chem 25: 299; (c) Hammes-Schiffer S, Tully JC (1994) J Chem Phys 101: 4657; (d) Sholl DS, Tully JC (1998) J Chem Phys 109: 7702
9. (a) Xiao L, Coker DF (1994) J Chem Phys 100: 8646; (b) Coker DF, Xiao L (1995) J Chem Phys 102: 496; (c) Mei HS, Coker DF (1996) J Chem Phys 104: 4755
10. (a) Webster F, Rossky PJ, Friesner PA (1991) Comput Phys Comm 63: 494; (b) Webster F, Wang ET, Rossky PJ, Friesner PA (1994) J Chem Phys 100: 483
11. Aleksandrov IV (1981) Z Naturforsch A 36: 902
12. Gerasimenko VI (1982) Teor Mat Fiz 150: 7
13. Boucher W, Traschen J (1988) Phys Rev D 37: 3522
14. (a) Zhang WY, Balescu R (1988) J Plasma Phys 40: 199; (b) Balescu R, Zhang WY (1988) J Plasma Phys 40: 215
15. Prezhdo OV, Kisil VV (1997) Phys Rev A 56: 162
16. (a) Martens CC, Fang J-Y (1996) J Chem Phys 106: 4918; (b) Donoso A, Martens CC (1998) J Phys Chem 102: 4291; (c) Kohen D, Martens CC (1999) J Chem Phys 111: 4343; (d) Kohen D, Martens CC (2000) J Chem Phys 112: 7345
17. Kapral R, Ciccotti G (1999) J Chem Phys 110: 8919
18. Schütte C (1999) preprint SC 99-10. Konrad-Zuse-Zentrum
19. Nielsen S, Kapral R, Ciccotti G (2001) J Chem Phys 115: 5805
20. Anderson A (1995) Phys Rev Lett 74: 621
21. Kantorovich LN (2002) Phys Rev Lett 89: 096105
22. (a) Jones KRW (1996) Phys Rev Lett 76: 4087; (b) Jones KRW (1992) Phys Rev D 45: R2590
23. (a) Wigner EP (1932) Phys Rev 40: 749; (b) Imre K, Özizmir E, Rosenbaum M, Zwiefel PF (1967) J Math Phys 5: 1097; (c) Hillery M, O'Connell RF, Scully MO, Wigner EP (1984) Phys Repts 106: 121.
24. Shiokawa K, Kapral R (2002) J Chem Phys 117: 7852
25. Sergi A, Kapral R (2003) J Chem Phys 118: 8566
26. Ando K (2002) Chem Phys Lett 360: 240
27. Horenko I, Saltzmann C, Schmidt B, Schütte C (2002) J Chem Phys 117: 11075
28. (a)Nielsen S, Kapral R, Ciccotti G (2000) J Chem Phys 112: 6543; (b) Nielsen S, Kapral R, Ciccotti G (2000) J Stat Phys 101: 225
29. Leggett AJ, Chakravarty S, Dorsey AT, Fisher MPA, Garg A, Zwerger M (1887) Rev Mod Phys 59: 1
30. Weiss U (1999) *Quantum dissipative systems*, World Scientific, Singapore
31. (a) Thompson K, Makri N (1999) J Chem Phys 110: 1343; (b) Makri N (1999) J Phys Chem B 103: 2823
32. Mac Kernan D, Ciccotti G, Kapral R (2002) J Chem Phys 116: 2346
33. Mac Kernan D, Ciccotti G, Kapral R (2002) J Phys Condens Matter 14: 9069
34. (a) Wan C, Schofield J (2002) J Chem Phys 113: 7047; (b) Wan C, Schofield J (2002) J Chem Phys 116: 494
35. Santer M, Manthe U, Stock G (2001) J Chem Phys 114: 2001
36. Martinez TJ, Ben-Nun M, Levine RD (1997) J Phys Chem A 101: 6389
37. Kapral R (2001) J Phys Chem A 105: 2885
38. Toutounji M, Kapral R (2001) Chem Phys 268: 79